First-Principles Calculations of Propane Dehydrogenation over PtSn Catalysts

ARTICLE *in* ACS CATALYSIS · MAY 2012

Impact Factor: 9.31 · DOI: 10.1021/cs300031d

ACS Catalysis

Research Article

pubs.acs.org/acscatalysis

First-Principles Calculations of Propane Dehydrogenation over PtSn Catalysts

Ming-Lei Yang,[†] Yi-An Zhu,*[,†] Xing-Gui Zhou,[†] Zhi-Jun Sui,[†] and De Chen*[,‡]

[†]State Key Laboratory of Chemical Engineering, East China University of Science and Technology (ECUST), Shanghai 200237, China

[‡]Department of Chemical Engineering, Norwegian University of Science and Technology (NTNU), N-7491 Trondheim, Norway

Supporting Information

ABSTRACT: Density functional theory calculations have been performed to investigate the effect of Sn on the catalytic activity and selectivity of Pt catalyst in propane dehydrogenation. Five models with different Sn to Pt surface molar ratios are constructed to represent the PtSn surfaces. With the increase of the Sn content, the *d*-band of Pt is broadened, which gives rise to a downshift in the *d*-band center on the PtSn surfaces. Consequently, the bonding strength of propyl and propylene on the alloyed surfaces is lowered. With the decomposition of the adsorption energy, the change in the surface deformation energy is predicted to be the dominant factor that determines the variation in the adsorption energy on the surface alloys, while on the bulk alloys the change in the binding energy makes a major contribution. The introduction of Sn lowers the energy barrier for propylene desorption and simultaneously increases the activation energy for propylene dehydrogenation, which has a positive effect on the selectivity toward propylene production. Considering the compromise between the catalytic activity and selectivity, the Pt_3Sn bulk alloy is the best candidate for propane dehydrogenation.

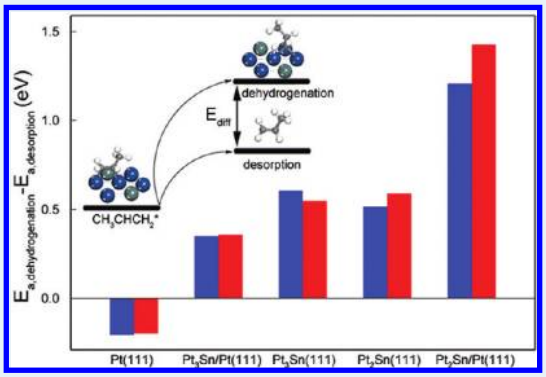

KEYWORDS: *PtSn, propane, dehydrogenation, selectivity, propylene*

INTRODUCTION

Sn has been widely used as an additive in heterogeneous catalysis over the past two decades to improve the catalytic performance of transition metals.[1−5] For instance, the alloy of Sn and Pt has been shown to have the capability of improving the catalyst selectivity and stability in propane dehydrogenation.[1] Experimentally, the introduction of Sn was found to increase the Pt dispersion and to decrease the ensemble size of the active sites, which in turn suppresses the side reactions such as the hydrogenolysis of C_3 intermediates.[6−11] An increase in the amount of coke deposition was also reported on PtSn catalysts, as compared to that on Pt.[3,12−14] Sn was believed to weaken the binding of the reactive intermediates with Pt and to transfer the coke precursors from the active Pt sites to the support, and consequently a long-term stability of PtSn catalysts is achieved.[3]

The chemisorption of C_3 intermediates on the Pt and PtSn surfaces has been examined in previous experimental and theoretical investigations.[15−20] Among them, propane and propylene have attained the most attention. Through reflection-absorption infrared spectroscopy (RAIRS), Zaera and Chrysostomou suggested that propylene favors the di-σ adsorption mode under low coverage over Pt(111), while above saturation coverage, a second layer of a weak adsorption mode, namely the π mode, was identified.[18] Recent density functional theory (DFT) calculations supported their findings and indicated that propylene is preferentially bonded to two Pt atoms at the bridge site with the propylene coverage lower than 0.25 ML.[15,19,20] The theoretical adsorption energy of propylene on the flat surfaces ranges from −0.50 eV to −0.93 eV, which can be attributed to different surface coverages and computational methods.[15,16,19,21] As for the PtSn alloyed catalysts, Tsai et al. performed a detailed temperature programmed desorption (TPD) and low energy electron diffraction (LEED) study on the adsorption of a series of alkenes and found that the desorption temperature of the adsorbed species shifts down with the increase of Sn content, which indicated that the presence of Sn weakens the binding strength between alkene and Pt.[17] More recently, first-principles calculations were performed to investigate the adsorption of propane and propylene over PtSn alloys.[16] Propane was found to be adsorbed on the surface without the formation of covalent bonds and a negligible change in the adsorption energy was observed from the Pt surface to the PtSn surface. As for propylene, the adsorption energy on the Pt_3Sn alloyed surface is much lower than that on Pt(111), in accordance with the experimental findings.[2,4,5,16]

Received: January 16, 2012
Revised: May 10, 2012
Published: May 14, 2012

   dx.doi.org/10.1021/cs300031d | ACS Catal. 2012, 2, 1247−1258

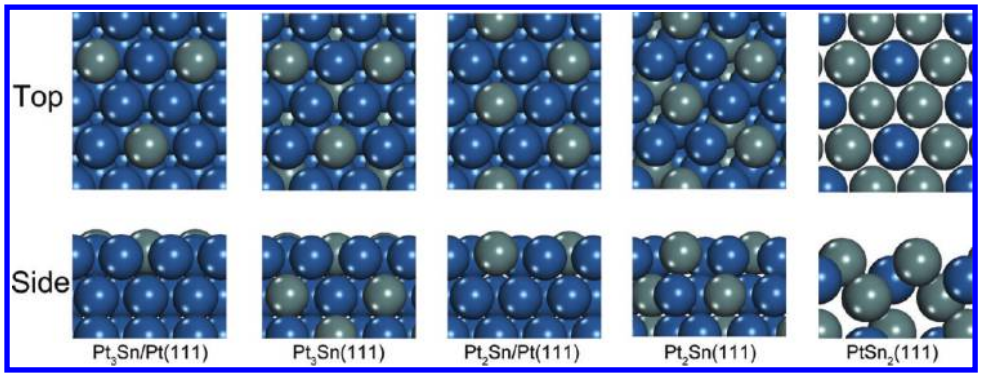

Figure 1. Top and side views of $Pt_3Sn/Pt(111)$, $Pt_3Sn(111)$, $Pt_2Sn/Pt(111)$, $Pt_2Sn(111)$, and $PtSn_2(111)$. Pt atoms are colored blue and Sn atoms are colored gray.

The production of propylene by propane dehydrogenation involves two elementary steps: propane to propyl followed by propyl to propylene. According to the reported kinetic parameters, the second dehydrogenation step was proposed to be the rate-determining step on both Pt and PtAu alloy.[22,23] Our previous DFT calculations showed that the activation barriers for these two steps were rather close on Pt(111), which also suggests that the second dehydrogenation step is the rate-determining step if the propane partial pressure is taken into account.[20] The experimental observations showed that the catalytic activity of PtSn catalysts [on a turnover frequency (TOF) basis] was about one-tenth as active as the Pt.[24] A similar trend was reported in cyclohexane dehydrogenation.[25] As no theoretical work has been performed to investigate the detailed reaction mechanism for propane dehydrogenation on PtSn catalyst so far, the physical origin of the key role of Sn remains elusive.

In propane dehydrogenation, the deep dehydrogenation and coke formation are the primary side reactions which strongly affect the selectivity toward propylene.[1,20] On the Pt catalyst, propylidyne that is produced by propylene dehydrogenation was captured using RAIRS.[26] Moreover, propyne was identified through the fluorescence yield near edge spectroscopy (FYNES) experiment, and it could be converted to propylidyne in the presence of H at room temperature.[27] On step sites, the deep dehydrogenated C_3 intermediates are more readily produced because of the stronger binding strength of propylene and lower energy barriers for subsequent dehydrogenation.[20] As compared to pure Pt, the PtSn alloys showed much higher selectivity toward propylene because the cracking and hydrogenolysis reactions were suppressed by the introduction of Sn.[1] In our previous work, the selectivity was defined as the activation energy difference between the dehydrogenation of propylene and the desorption of propylene.[20] Thus, the understanding of the effect of Sn content on the activation energy difference is of vital importance.

This paper is organized as follows. In section 2, details of the computational methods and the strategy to construct the models for the PtSn alloyed surfaces are described. In section 3, we present the calculated results of the adsorption energies, the energy barriers for the dehydrogenation and cracking of the C_3 intermediates on the PtSn surfaces. To gain insight into the physical origin of the key role of Sn in propane dehydrogenation, we analyze the electronic properties of the surface Pt atoms over alloys as well as the geometric and coverage effects on the surface catalytic activity and selectivity toward propylene. Finally, we summarize the conclusions in the last section.

COMPUTATIONAL DETAILS

In the present work, all the total energy DFT calculations were carried out with the VASP package,[28−30] where Kohn−Sham equations are solved self-consistently with the generalized gradient approximation (GGA) functional proposed by Perdew, Burke, and Ernzerhof.[31] As the GGA functional underestimates the binding, uncertainties of 0.1 eV exist in the DFT calculated adsorption energies.[31] A plane wave energy cutoff of 400 eV was used in these calculations to achieve a tight convergence. The interactions between valence electrons and ion cores were represented by Blöchl's all-electron-like projector augmented wave method (PAW),[32] which regards the 6s 5d states as the valence configuration for Pt, 5s 5p states for Sn, 2s 2p states for C, and 1s state for H. Brillouin zone sampling was performed by using a Monkhorst−Pack grid with respect to the symmetry of the system, and the electronic occupancies were determined according to the Methfessel−Paxton scheme[33] with an energy smearing of 0.2 eV. The dipole correction is not included because it changes the total energy of the PtSn surface by less than 0.04 eV and had negligible effect on the geometries of the adsorption configurations.

Experimentally, the well-defined PtSn alloys were obtained by Sn vapor deposition, followed by annealing.[34,35] Through the LEED and scanning tunneling microscopy (STM) studies, the structure of the PtSn alloys with the Sn to Pt surface molar ratios of 1/3 and 1/2 were detected.[34−39] On the other hand, the $PtSn_2$ bulk alloy has been captured by X-ray diffraction (XRD).[40] Therefore, the models with the Sn to Pt surface molar ratios of 1/3, 1/2, and 2 were constructed to represent the surface structures of the PtSn catalysts. The segregation energies of Sn from bulk Pt to Pt surface were first calculated at different Sn coverages (see Supporting Information for details). It was found that Sn atoms prefer to stay on the Pt(111) surface to form a surface alloy at the Sn coverages lower than 1/4 ML while PtSn bulk alloy is favored at higher Sn contents. As the small magnitudes of the segregation energies at the Sn coverage of 1/4 and 1/3 ML indicate moderate segregation and antisegregation, both bulk and surface alloys were taken into account for Pt_3Sn and Pt_2Sn in this study. Then the five alloyed surfaces which are derived from the surface alloys [$Pt_3Sn/Pt(111)$ and $Pt_2Sn/Pt(111)$] and the bulk alloys [$Pt_3Sn(111)$, $Pt_2Sn(111)$, and $PtSn_2(111)$] were constructed, as illustrated in Figure 1.

dx.doi.org/10.1021/cs300031d | ACS Catal. 2012, 2, 1247−1258

Table 1. Adsorption Energies and Equilibrium Adsorption Height (H···Pt) of Propane on Pt and PtSn Surfaces

	experimental data[45−47] (eV)	Nykänen et al.[16] (eV)	PBE functional (eV)	vdW-DF functional (eV)	H···Pt (Å)
Pt(111)[19]	−0.35 ∼ −0.44	−0.37	−0.04	−0.42	3.23
Pt_3Sn/Pt(111)		−0.34	−0.02	−0.41	3.36
Pt_3Sn(111)		−0.33	−0.02	−0.38	3.74
Pt_2Sn/Pt(111)			−0.02	−0.42	3.45
Pt_2Sn(111)			−0.08	−0.36	3.62
$PtSn_2$(111)		−0.28	−0.02	−0.30	4.13

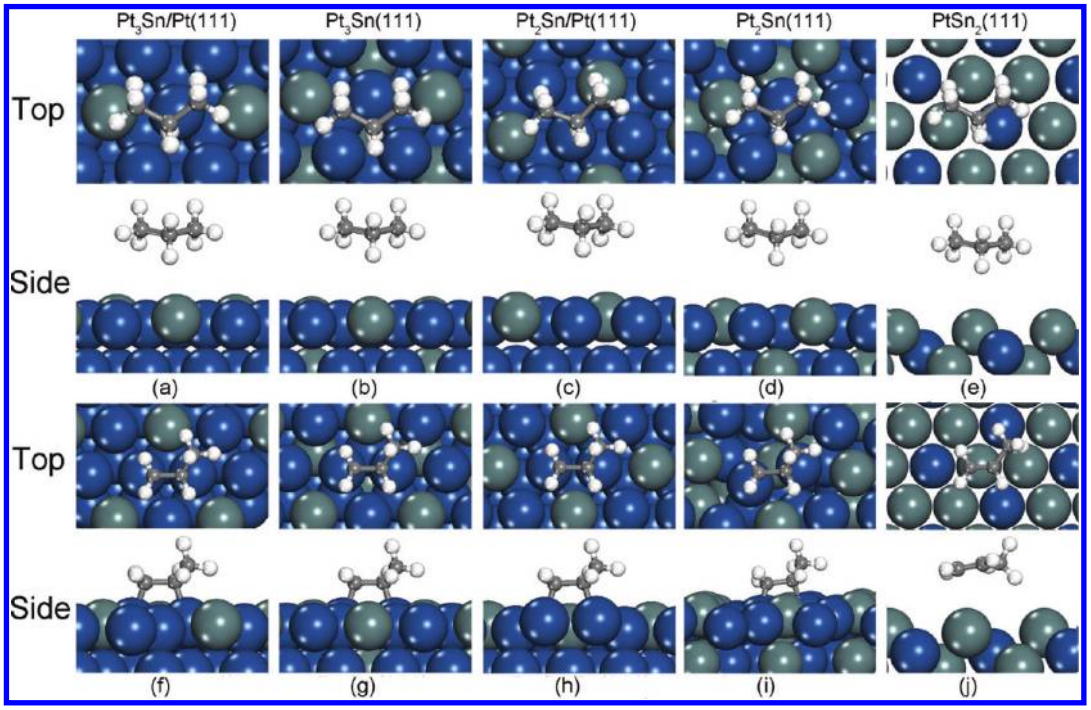

Figure 2. Top and side views of the adsorption configurations of propane (a to e) and propylene (f to j) on the PtSn alloyed surfaces.

For the first layer of the Pt_3Sn and Pt_2Sn alloys, the Sn and Pt atoms are in the same plane with a slight upward relaxation of Sn atoms (0.19−0.29 Å), which is in good agreement with the earlier DFT calculations and experimental observations.[2,34] In our calculations, a four-layer slab with a $(2\sqrt{3} \times 2\sqrt{3})R30°$ supercell was used to represent the Pt_3Sn and Pt_2Sn alloyed surfaces, achieving the coverage of adsorbates of 1/12 ML. The successive slabs were separated by a vacuum region as thick as 12 Å to eliminate periodic interactions. The Monkhorst−Pack k-mesh contains three k-points in the *x*- and *y*-direction and one k-point in the *z*-direction. The bottom two layers of the slab were kept fixed to their crystal lattice positions. The $PtSn_2(111)$ surface is derived from the fluorite crystal structure,[16,41] and a k-mesh of 5 × 5 × 1 was used to sample the k-points in the surface Brillouin zone. The ground-state geometries of bulk and surfaces were obtained by minimizing the Hellman−Feynman forces with the conjugate-gradient algorithm until the force on each ion is below 0.03 eV/Å.

The adsorption energy of an adsorbate, E_{ads}, was calculated as follows:

$$E_{ads} = E_{adsorbate/surface} - E_{adsorbate} - E_{surface} \quad (1)$$

where $E_{adsorbate/surface}$ is the total energy of interacting system of the PtSn surface and adsorbate; $E_{surface}$ and $E_{adsorbate}$ are the DFT total energies of bare surface and adsorbate in vacuum, respectively. A negative E_{ads} corresponds to an energy gain process. For propane adsorption, the vdW-DF implemented in VASP is performed to include the dispersion interactions.

Transitional states (TS) were located with the dimer method.[42−44] The most stable configurations of the reactant on the surface were determined by the standard DFT minimization. These configurations were used as the initial state, from which the dimer method was used to find the lowest curvature mode and to climb up the potential energy surface from minima to saddle points. The convergence was regarded to be achieved when the force on each atom was less than 0.03 eV/Å. All the saddle points identified in this work were confirmed by frequency calculations. Only one imaginary frequency was obtained at each saddle point.

RESULTS AND DISCUSSION

Adsorption on PtSn Surfaces. *Propane Adsorption.* The adsorption energies of propane on all the Pt and PtSn surfaces calculated by PBE and vdW-DF functionals are summarized in Table 1. According to the GGA-PBE results, the molecular propane is weakly adsorbed on the PtSn surfaces, and the equilibrium adsorption heights are in the range from 3.2 to 4.0 Å, as shown in Figure 2. The optimized bond parameters of the adsorbed propane are almost identical to the gas-phase propane. According to the previous local density of states (LDOS) analysis, there is no hybridization between propane and Pt states.[16] This suggests that propane is not covalently adsorbed on the PtSn surfaces. The adsorption energies

dx.doi.org/10.1021/cs300031d | ACS Catal. 2012, 2, 1247−1258

Table 2. Calculated Frequencies of the Vibrational Modes When Propane Is Adsorbed on the Pt and PtSn Surfaces (cm^{-1})

mode	Pt(111)	Pt_3Sn/Pt(111)	Pt_3Sn(111)	Pt_2Sn/Pt(111)	Pt_2Sn(111)	$PtSn_2$(111)	gas phase
CH_3_s_st[a]	2962	2955	2966	2950	2959	2968	2964
CH_3_as_st[b]	3037	3048	3039	3042	3041	3039	3041
CH_2_s_st	2950	2854	2872	2864	2892	2958	2961
CH_2_as_st	2979	2976	2984	2983	2978	2983	2986

[a]The letter "s" is short for "symmetric" and "st" for "stretching". [b]The letters "as" are short for "asymmetric".

Table 3. Adsorption Energies of 1-Propyl, 2-Propyl, And Propylene on Pt and PtSn Surfaces (eV)

	Pt(111)[19]	Pt_3Sn/Pt(111)	Pt_3Sn(111)	Pt_2Sn/Pt(111)	Pt_2Sn(111)	$PtSn_2$(111)
1-propyl	−1.88	−1.63	−1.74	−1.59	−1.58	−1.47
2-propyl	−1.67	−1.38	−1.44	−1.37	−1.30	−1.26
propylene	−0.97	−0.52	−0.50	−0.42	−0.61	−0.05

obtained by GGA-PBE calculations on all the PtSn surfaces are in the range from −0.02 to −0.08 eV, which are in the typical range of weak physisorption.

The molecular beam and TPD experiments, however, demonstrated that the adsorption of propane on Pt(111) is moderately exothermic, and the adsorption energies are measured in the region of −0.35 ∼ −0.44 eV.[45−47] The considerable discrepancy could be explained by the poor description of the van der Waals interaction by the PBE functional, as evidenced by Nykänen and Honkala who claimed that the adsorption energies of propane on PtSn surfaces become more negative once the conventional Kohn−Sham DFT energies have been corrected by using a nonlocal correlation functional.[16,48] Here we employed the vdW-DF functional proposed by Dion et al. to account for the London dispersion force between propane and metal surfaces.[49] While this functional was reported to overestimate the van der Waals interaction by 0.15 eV in energy, it shows significant improvement in the depiction of the adsorption of non-covalently bound complex compared to other functionals.[48,49] With this correction, the calculated adsorption energies fall well within the range of −0.30 ∼ −0.42 eV (see Table 1), in good agreement with the experimental data.[45−47]

To further shed light on the adsorption of propane on the Pt and PtSn surfaces, the frequencies of the vibrational modes were computed on the basis of the optimized adsorption configurations. As for the saturated hydrocarbons, the vibration mode softening which arises from the interaction between the C−H bond and the metal surface is observed through RAIRS spectra studies, and the "softened" C−H stretching frequency occurs commonly at 2700−2900 cm^{-1}.[50−52] From Table 2, the comparison between the vibrational frequencies of propane in the gas phase and those in the adsorbed state suggests that the symmetric CH_2 stretching mode makes a major contribution to the vibrational mode softening, indicating that the C−H bonds in the physisorbed propane are weakened upon adsorption even if no covalent bond is formed between propane and metal surfaces.

1-Propyl and 2-Propyl Adsorption. Both 1-propyl and 2-propyl are coordinated to a surface atom at the atop site on all the PtSn surfaces. As for the Pt_3Sn and Pt_2Sn alloy surfaces, the adsorption of 1-propyl and 2-propyl on Pt atoms is energetically more favorable than that on Sn, as evidenced by the more negative adsorption energies. On $PtSn_2$(111), however, propyl isomers prefer to be bound to a Sn atom because the outermost Pt atoms reside deeper in the surface. As shown in Table 3, the adsorption energy of 1-propyl on Pt(111) is calculated to be −1.88 eV, more negative than those on the alloy surfaces. This indicates that the alloying of Pt with Sn weakens the reactivity of surface Pt atoms. The binding strength decreases with increasing Sn content: Pt(111) > Pt_3Sn > Pt_2Sn > $PtSn_2$. Furthermore, the adsorption energies of 1-propyl on the PtSn surfaces are generally 0.20−0.30 eV more negative than those of 2-propyl, and therefore it is reasonable to expect that the C−H bond cleavage at the methyl group of propane is kinetically more favorable with the consideration of the BEP relationship.[53−55]

Propylene Adsorption. The adsorption of propylene is investigated by assigning a molecule at the bridge and atop sites, which are known as the di-σ and π adsorption modes, respectively. On the Pt_3Sn and Pt_2Sn alloyed surfaces, the di-σ mode was found to be energetically more favorable, in accordance with the findings of the previous LEED analysis and DFT investigations.[20,56] The alloy surface contains two different bridge sites, Pt−Pt and Pt−Sn. The Pt−Pt bridge site is more favorable for propylene adsorption. Two types of bridge sites are present on the alloyed surfaces: the Pt−Pt and Pt−Sn bridges. The Pt−Pt bridge site is energetically more favorable to accommodate propylene, and the molecule propylene positioned initially at the Pt−Sn bridge site will be relaxed to the Pt−Pt bridge site upon geometry optimization. The C═C bond length in propylene is elongated by about 0.15 Å upon adsorption, signifying that the C═C bond is weakened by the formation of the covalent bonds between propylene and Pt atoms. The adsorption energies of propylene on Pt_3Sn and Pt_2Sn vary from −0.42 to −0.61 eV, much less negative than that on Pt(111).[15,20] The activation energy for propylene desorption on Pt_3Sn has been measured to be 0.6 eV through TPD experiments, very close to our calculated adsorption energies.[17] On $PtSn_2$(111), propylene is physisorbed without the formation of covalent bonds, as shown in Figure 2. The adsorption energy is calculated to be −0.36 eV by using the vdW-DF functional. The C═C double bond is measured to be 1.34 Å, which is almost identical to that of propylene in the gas phase.

Activity for Propane Dehydrogenation. The elementary steps including both the C−H and the C−C bond cleavage in propane dehydrogenation are shown in Scheme 1. The dehydrogenation reactions can be divided into two groups. The first group consists of the dehydrogenation steps from propane to propylene (Steps 1−4), and the energy barriers for these four steps are good descriptors for the catalytic activity of alloyed surfaces toward propylene production. The second group contains the deep dehydrogenation steps of propylene,

Scheme 1. Reaction Network for Propane Dehydrogenation to Propenyl[a]

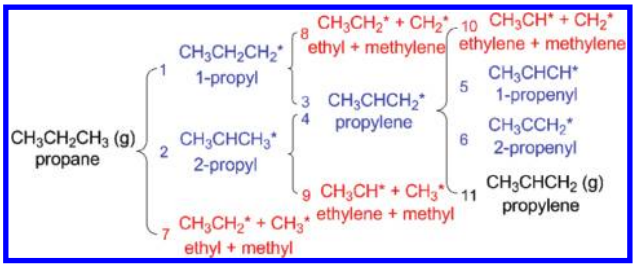

[a]The detached H atoms are not included for clarity. The numbers signify the sequence numbers of the elementary steps.

namely, Steps 5 and 6, and the activation energy difference between these two steps and propylene desorption is traditionally used to evaluate the selectivity toward propylene. It should be noted that the reactions on $PtSn_2(111)$ were not taken into account because the Pt atoms on this alloyed surface are inactive for the adsorption of the reaction intermediates.

C−H Bond Activation. In our calculations, the most stable adsorption configurations are assigned to be the initial states for the dehydrogenation reactions. The detached H atom is assumed to be transferred to a location that is infinitely far away from the C_3 intermediates. This enables us to neglect the coadsorption effect of hydrogen, which is generally defined as the repulsive interaction energy between H and C_3 intermediates in the coadsorption configurations. For instance, the interaction energy between the coadsorbed H and propylene is calculated to be 0.08 eV.

The geometries of the transition states for the dehydrogenation steps are schematically represented in Figure 3, where the lengths of the activated C−H bonds are also given. From the figure, some general trends are observed: (1) In the activated complex, the monovalent groups (1-propyl and 2-propyl) prefer to be bound to the atop site, and the divalent group, namely, propylene, is bonded to the bridge site, which is in good agreement with the findings in C_1 hydrogenation.[57−59] The H atom that is detached from the C_3 intermediates is relaxed to the atop or bridge site. (2) On all the alloyed surfaces the geometries of these transition states resemble those of the final states; that is, the transition state is close to the final state on the potential energy surface. (3) The introduction of Sn has a minor effect on the structures of the transition states. For instance, the lengths of the activated C−H bond for Step 6 on the PtSn alloyed surfaces are almost identical to that on Pt(111) (1.55 Å).[20]

The energy barriers for the dehydrogenation reactions are summarized in Table 4. To facilitate comparison, the corresponding data on Pt(111) are also included. From the table, one can see that the energy barriers for the activation of both propane and propyl become higher with increasing Sn content, which fall within the regions of 0.74−1.25 eV and 0.63−1.10 eV on the alloyed surfaces, respectively. According to the Arrhenius equation, it can be estimated that a change of 0.40 eV in activation energy [e.g., the dehydrogenation of propane toward 1-propyl goes from the Pt(111) surface to the $Pt_2Sn(111)$ surface] will change the rate constant by 200 times. Therefore, alloying Pt with Sn will significantly lower the reaction rate of propane dehydrogenation, in accordance with the experimental observations.[24] Figure 4 shows the energy profiles for the dehydrogenation process from propane to propylene on both the Pt and PtSn surfaces. On $Pt_2Sn(111)$ the activation of propane is suggested to be the rate-determining step because the point with the highest potential energy usually defines a slowest step in such an energy diagram, whereas on the other PtSn surfaces the activation of propyl determines the overall reaction rate.

It should be noted in Figure 4 that while there is a considerable discrepancy between the activation energy for Step 1 on $Pt_3Sn/Pt(111)$ and that on $Pt_3Sn(111)$, the corresponding reaction energies are rather close. This finding is in conflict with the well-known BEP relationship, which claims that there is a linear relationship between the activation energies (E_{act}) for elementary steps and the reaction heats if entropy effects are neglected:

$$E_{act} = E_0 + \alpha \Delta H \qquad (0 < \alpha < 1) \tag{2}$$

Figure 5a shows the plot of the activation energy for Step 1 against the reaction energy over the Pt and PtSn surfaces, which does not give a straight line. To provide a rational interpretation, the activation energy is decomposed as follows:[60]

$$E_{act} = E_{bond(C_3H_7-H)} + E_{ads,TS} \tag{3}$$

where $E_{ads,TS}$ is the adsorption energy of the activated complex with respect to the gaseous 1-propyl and H species and $E_{bond(C_3H_7-H)}$ is the C−H bond energy at the methyl group of gaseous propane. As the bond energy keeps constant, the variation in E_{act} depends solely on the change in $E_{ads,TS}$ which can be further decomposed into the following three terms:

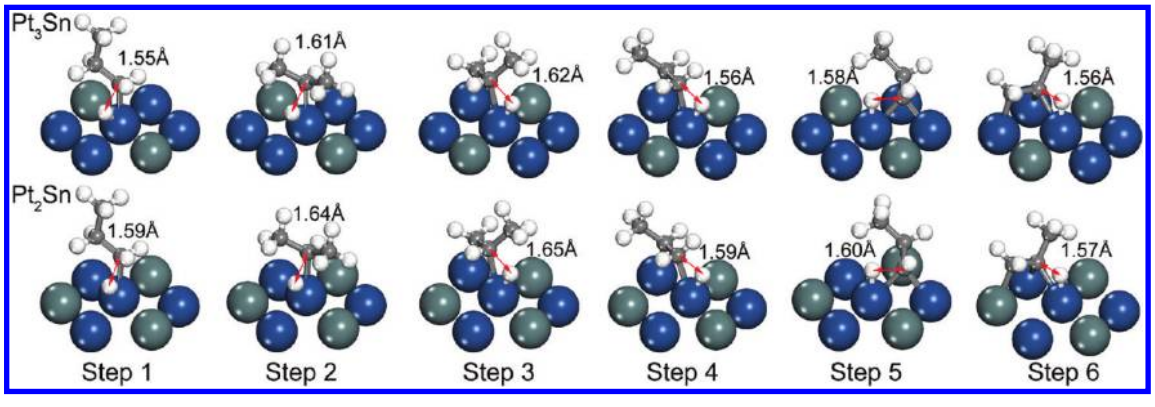

Figure 3. Geometries of the transition states for the dehydrogenation of propane, propyl isomers, and propylene on the Pt_3Sn and Pt_2Sn alloys.

dx.doi.org/10.1021/cs300031d | ACS Catal. 2012, 2, 1247−1258

Table 4. Energy Barriers for Propane Dehydrogenation on the Pt(111) and PtSn Surfaces (eV)

	reaction	Pt(111)[20]	Pt_3Sn/Pt(111)	Pt_3Sn(111)	Pt_2Sn/Pt(111)	Pt_2Sn(111)
Step 1	$CH_3CH_2CH_3$ (g) → $CH_3CH_2CH_2$* + H*	0.69	0.97	0.75	1.22	1.10
Step 2	$CH_3CH_2CH_3$ (g) → CH_3CHCH_3* + H*	0.70	1.00	0.78	1.25	1.17
Step 3	$CH_3CH_2CH_2$* → CH_3CHCH_2* + H*	0.70	0.86	0.74	1.08	0.69
Step 4	CH_3CHCH_3* → CH_3CHCH_2* + H*	0.68	0.84	0.87	1.10	0.63
Step 5	CH_3CHCH_2* → CH_3CHCH* + H*	0.76	0.87	1.11	1.63	1.12
Step 6	CH_3CHCH_2* → CH_3CCH_2* + H*	0.77	0.88	1.05	1.85	1.20

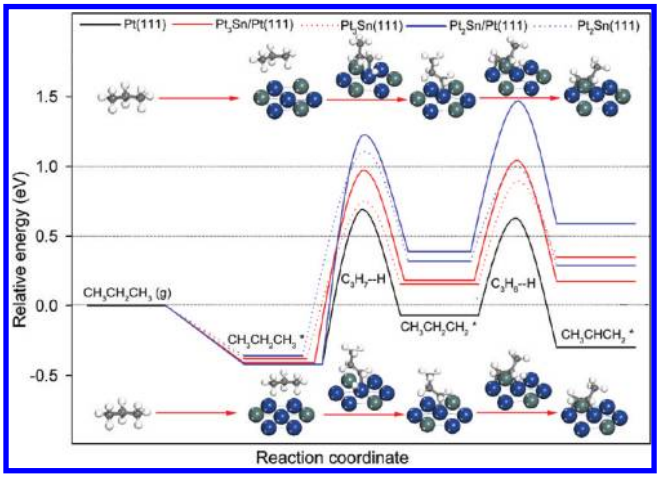

Figure 4. Energy profiles for propane dehydrogenation to propylene on Pt and PtSn surfaces.

$$E_{ads,TS} = E_{ads,TS(1-propyl)} + E_{ads,TS(H)} + E_{int,lat(H,1-propyl)} \quad (4)$$

where $E_{ads,TS(1-propyl)}$ $[E_{ads,TS(H)}]$ is the adsorption energy of 1-propyl (H) with its geometry in the activated complex and $E_{int,lat(H,1-propyl)}$ represents the interaction energy between H and 1-propyl in the activated complex. From eq 4, one can see that a more negative $E_{ads,TS(1-propyl)}$ $[E_{ads,TS(H)}]$ and a lower $E_{int,lat(H,1-propyl)}$ lead to a more negative $E_{ads,TS}$, which in turn gives rise to a lower energy barrier.

The decomposition of the activation energy for Step 1 on Pt(111), Pt_2Sn(111), Pt_2Sn/Pt(111), Pt_3Sn(111), and Pt_3Sn/Pt(111) are summarized in Table 5. Then the activation energy for Step 1 is plotted against $E_{ads,TS(H)}$, $E_{ads,TS(1-propyl)}$ and $E_{int,lat(H,1-propyl)}$, as shown in Figure 5. One can see that only for the plot of E_{act} against $E_{ads,TS(H)}$ does a straight line appear, and more importantly, the slope of the line is close to unity; that is, the variation in $E_{ads,TS(H)}$ is suggested to make a major contribution to the change in E_{act}. Therefore, the lower activation energy for Step 1 on Pt_3Sn(111) is attributed primarily to the strengthened binding of H to Pt compared to that on the Pt_3Sn/Pt(111) surface. Similar findings have been reported by Goda et al. who found that the activation barriers for ethyl and vinyl dehydrogenation scale approximately linearly with the H binding energies.[61]

C−C Bond Activation. In propane dehydrogenation, the cracking of C_3 derivatives leads to the formation of the undesired byproducts such as ethylene, methane, and coke. The selectivity toward these products on PtSn catalysts is in the range from 10% to 20%, as reported by experimental observations.[1] Here the cracking of propane, propyl, and propylene is investigated to examine the competition between C−H and C−C bond breaking. The obtained structures of the transition states for the four elementary steps on the PtSn surfaces are shown in Figure 6, which are found to have similar geometries to those on Pt(111).[20] In the transition state for propane cracking the methyl and ethyl groups are located at the atop site, while at the saddle points for propyl and propylene cracking an atop and a bridge site are involved in the active centers. The energy barriers for these reactions are listed in Table 6. From the table, it can be seen that the cracking of the C_3 intermediates is mostly kinetically more unfavorable on the PtSn surfaces than that on Pt(111), and all the activation energies for C−C bond cleavage are higher than 1.30 eV. Carefully analyzing the competition between the activation of C−H bond and C−C bond for each intermediate, we find that the cracking of these four species are kinetically hindered because of the much higher energy barriers.

According to our previous DFT calculations,[20] propylene tends to be deep dehydrogenated until propyne is produced, the cracking of which leads to the formation of the side products. As compared to the Pt(111) surface, the PtSn alloyed surfaces have lower catalytic activity for the C−H bond cleavage of C_3 intermediates, and consequently the formation of the deep dehydrogenated intermediates turns kinetically unfavorable. Therefore, the inhibition of cracking on the PtSn alloys might be largely due to the suppression of the deep dehydrogenation steps, which gives rise to a higher selectivity toward propylene.

Selectivity toward Propylene on PtSn Surfaces. In propane dehydrogenation, the deep dehydrogenation of propylene, followed by the cracking of the deep dehydrogenated intermediates, has an negative effect on the selectivity toward propylene production. Thus, the competition between propylene dehydrogenation and propylene desorption is investigated to gain a better understanding of the key role of Sn in improving the catalyst selectivity. Figure 7a shows the calculated equilibrium constants for propylene desorption at 1 atm as the temperature increases from 700 to 900 K (see Supporting Information for details). The desorption of propylene shows the highest and lowest equilibrium constants on Pt_3Sn(111) and Pt(111), respectively, which indicates that propylene is far less stable on the PtSn surfaces than that on Pt(111).

Figure 7b summarizes the energy barrier differences between propylene dehydrogenation and propylene desorption over the Pt(111) and PtSn surfaces. A positive value indicates desorption is preferred. On Pt(111), the energy barrier for the deep dehydrogenation of propylene is 0.28 eV lower than that for propylene desorption. According to the Arrhenius equation, the rate constant for propylene desorption ($k_{desorption}$) is 1/15 of that for propylene dehydrogenation (k_{dehy}) under experimental conditions, leading to a low selectivity toward propylene. The introduction of Sn lowers the desorption barrier of propylene to the gas phase and simultaneously increases the energy barrier for deep dehydrogenation, which gives rise to much higher $k_{desorption}$ than k_{dehy} on the PtSn

dx.doi.org/10.1021/cs300031d | ACS Catal. 2012, 2, 1247−1258

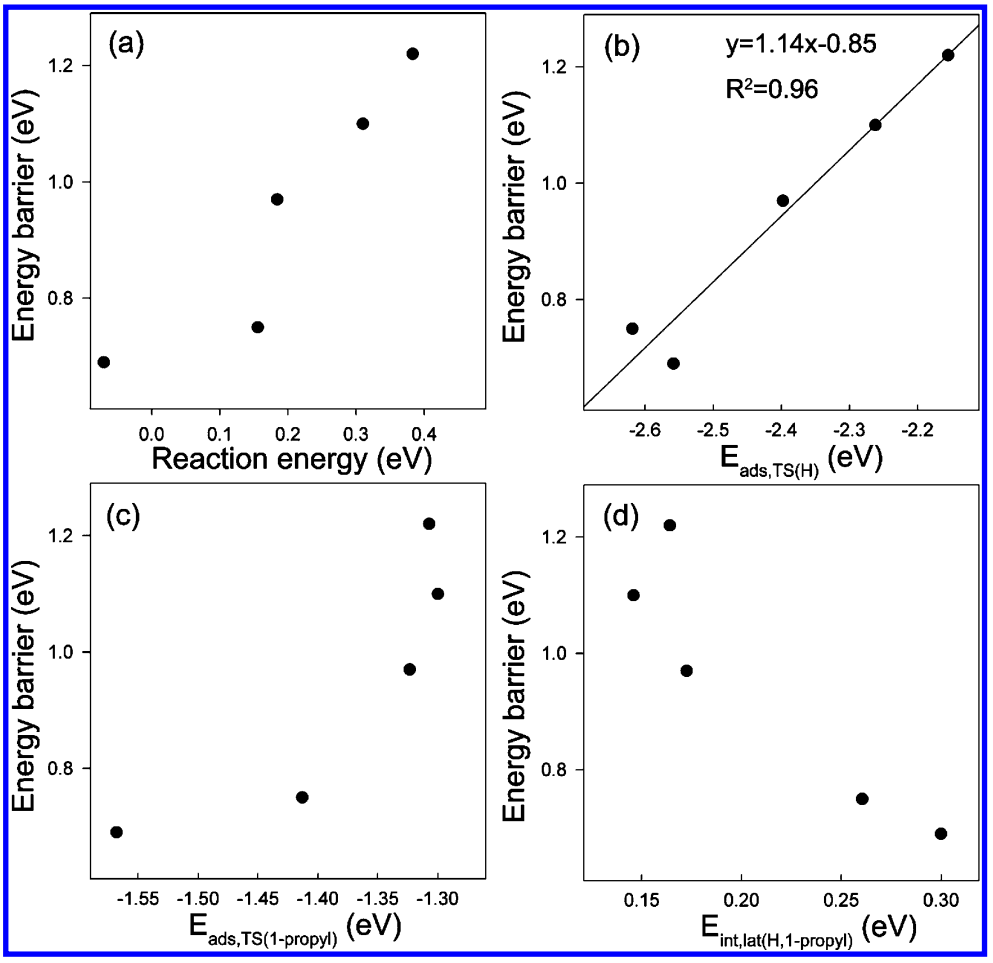

Figure 5. Plots of E_{act} for Step 1 against (a) the reaction energy, (b) $E_{ads,TS(H)}$, (c) $E_{ads,TS(1-propyl)}$, and (d) $E_{int,lat(H,1-propyl)}$ over the Pt and PtSn surfaces.

Table 5. Decomposition of the Activation Energy for Propane Dehydrogenation (Step 1) on Pt(111), Pt_3Sn, and Pt_2Sn Surfaces (eV)

surface	$E_{ads,TS}$	$E_{ads,TS(H)}$	$E_{ads,TS(1-propyl)}$	$E_{int,lat(H,1-propyl)}$
Pt(111)	−3.83	−2.56	−1.57	0.30
Pt_3Sn/Pt(111)	−3.55	−2.40	−1.32	0.17
Pt_3Sn(111)	−3.77	−2.62	−1.41	0.26
Pt_2Sn/Pt(111)	−3.30	−2.16	−1.31	0.16
Pt_2Sn(111)	−3.42	−2.26	−1.30	0.15

surfaces. For example, $k_{desorption}$ is about 120 times greater than k_{dehy} on Pt_3Sn/Pt(111). As a result, the selectivity toward propylene on the PtSn surfaces is predicted to be much higher

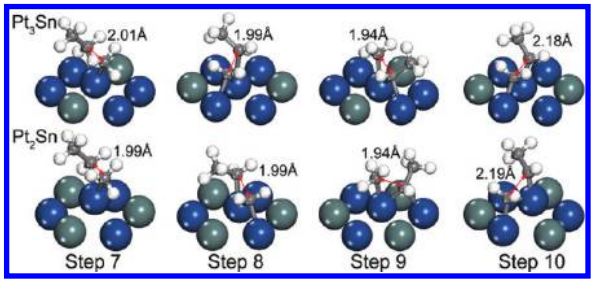

Figure 6. Geometries of the transition states for the C−C bond cleavage of propane, propyl, and propylene on the PtSn alloys.

than that on Pt(111), as evidenced by the experimental observations.[1] Moreover, the energy barrier for propylene dehydrogenation is more sensitive to the Sn content, and the best selectivity is achieved on Pt_2Sn/Pt(111). However, the high selectivity is attained at the expense of the catalytic activity for propane activation, as indicated in Table 4. Therefore, considering the compromise between the catalytic activity and selectivity, the Pt_3Sn bulk alloy is the best candidate for propane dehydrogenation.

Origin of the Surface Reactivity and Selectivity. Among the Pt and PtSn alloyed surfaces, Pt(111) is found to be most active for propane dehydrogenation at low coverages. The PtSn alloyed surfaces suffer from higher energy barriers for the dehydrogenation of the C_3 intermediates, which gives rise to low reaction rate for propane activation. On the other hand, through the examination of the activation energy difference between propylene dehydrogenation and propylene desorption, we find that the selectivity toward propylene on the PtSn alloy surfaces is higher than that on Pt(111). To elucidate the relationship between catalytic activity and selectivity, the physical origin of the catalytic behavior of Pt-based catalysts is then examined.

Correlation of Catalytic Activity with Surface d-Band Center. The projected density of states onto the *d*-bands of the surface Pt atoms on the Pt(111) and PtSn alloyed surfaces is shown in Figure 8a, and the *d*-band centers defined within the framework of the Hammer−Nørskov model are calculated and

dx.doi.org/10.1021/cs300031d | ACS Catal. 2012, 2, 1247−1258

Table 6. Energy Barriers for the C−C Bond Cleavage of the C_3 Intermediates on the Pt(111) and PtSn Surfaces (eV)

	reaction	Pt(111)[20]	Pt_3Sn/Pt(111)	Pt_3Sn(111)	Pt_2Sn/Pt(111)	Pt_2Sn(111)
Step 7	$CH_3CH_2CH_3(g) \rightarrow CH_3CH_2^* + CH_3^*$	2.40	2.64	2.42	2.65	2.38
Step 8	$CH_3CH_2CH_2^* \rightarrow CH_3CH_2^* + CH_2^*$	1.58	1.85	2.02	2.07	1.40
Step 9	$CH_3CHCH_3^* \rightarrow CH_3CH^* + CH_3^*$	1.71	1.91	1.70	2.16	1.35
Step 10	$CH_3CHCH_2^* \rightarrow CH_3CH^* + CH_2^*$	1.66	2.14	2.09	2.24	1.84

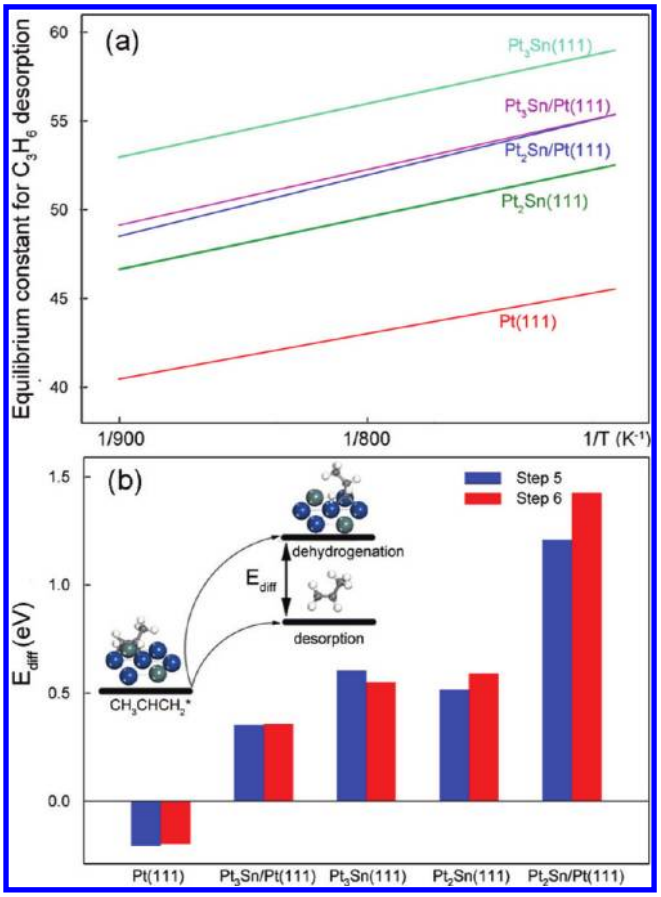

Figure 7. (a) Equilibrium constant for propylene desorption on the Pt and PtSn surfaces; (b)energy barrier difference (E_{diff}) between propylene dehydrogenation and propylene desorption over the Pt(111) and PtSn surfaces.

given in Table 7.[62] With the increase in Sn content, the *d*-band centers of surface Pt atoms are shifted farther below the Fermi

Table 7. *d*-Band Electronic Structure of Pt on the Pt and PtSn Alloyed Surfaces

surface	f_d	ε_d (eV)	W (eV)	ε_d by Delbecq et al.[2] (eV)
Pt(111)	0.88	−1.95	2.47	−1.93
Pt3Sn/Pt(111)	0.88	−2.12	2.66	−2.09
Pt3Sn(111)	0.90	−2.06	2.55	
Pt2Sn/Pt(111)	0.90	−2.16	2.67	−2.12
Pt2Sn(111)	0.91	−2.18	2.71	

level, as reported in the earlier DFT studies.[2,16] To gain a better understanding of the role of Sn in the adsorption and catalytic properties of the PtSn alloys, the binding energy of 1-propyl and the activation energy for propane dehydrogenation (Step 1) are related with the *d*-band centers of surface Pt atoms, as shown in Figure 8b. As one might expect, an upshift of the *d*-band center gives rise to a stronger binding of 1-propyl to the surface and a lower energy barrier for propane dehydrogenation. In particular, the correlation between the binding energy of 1-propyl and the *d*-band center exhibits a good linear relationship. On the other hand, the correlation between the activation energies for Step 1 and the *d*-band centers does not give a straight line. Nevertheless, the relationship indicates that the introduction of Sn leads to a downshift of the *d*-band center, which in turn lowers the catalytic activity for propane dehydrogenation.

According to the simple rectangular form of the *d*-band, the position of the *d*-band center (ε_d) is related both to the bandwidth ($\bar{W}$) and to the band filling (f_d):[63]

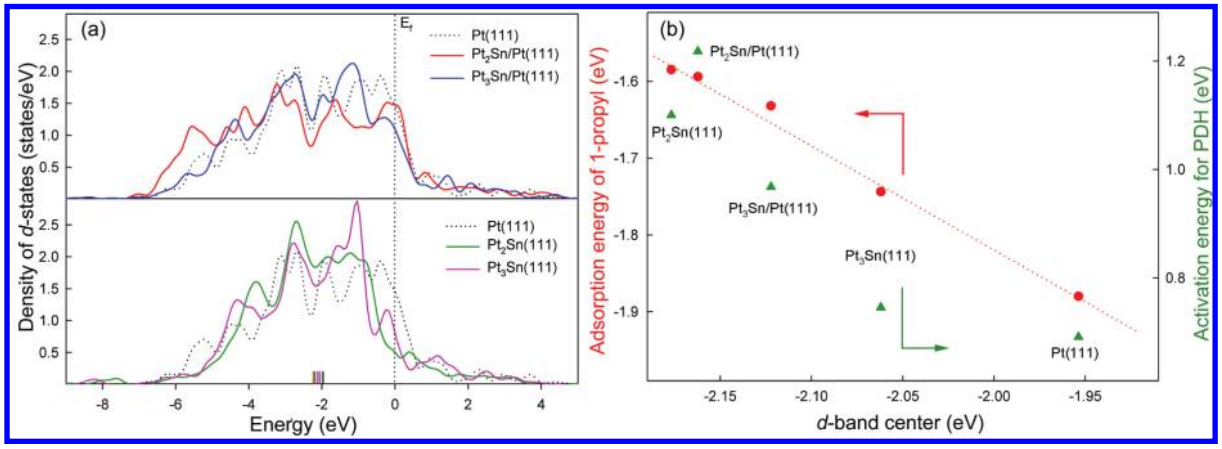

Figure 8. (a) DOS projected onto the *d*-bands of surface Pt atoms on the Pt and PtSn surfaces. The small vertical indicators above the *x*-axis signify the *d*-band centers; (b) plots of the binding energies of 1-propyl (red dots) and the energy barriers for Step 1 (green dots) against the *d*-band centers.

dx.doi.org/10.1021/cs300031d | ACS Catal. 2012, 2, 1247−1258

$$\bar{W}^2 = \frac{1}{3}\left(\frac{1}{0.5 - f_d}\varepsilon_d\right)^2 (1 - 3f_d + 3f_d^2) \quad (5)$$

Table 7 lists the calculated values of these three quantities on the Pt and PtSn surfaces. As the *d*-band filling is almost conserved, the *d*-bandwidth plays a key role in determining the *d*-band center. A linear relationship between the *d*-band center and the *d*-bandwidth is identified, as shown in Figure 9.

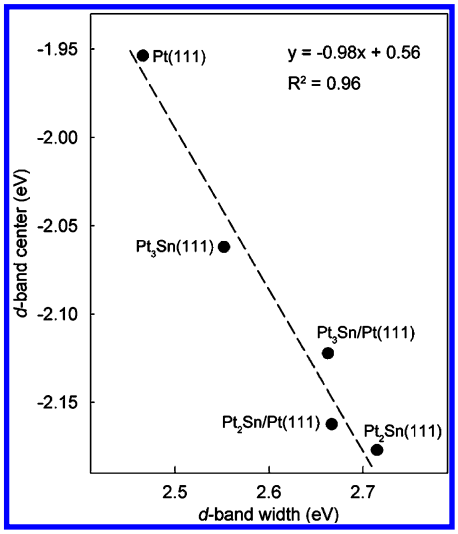

Figure 9. Linear relationship between the *d*-band center and the *d*-bandwidth.

Deviations from the straight line can be traced to the minor change in the *d*-band filling. As the *d*-band is broadened, the *d*-band center shifts downward to maintain the *d*-band filling. Therefore, it is reasonable to conclude that the alloying of Pt with less reactive Sn leads to the increase in the *d*-bandwidth, which gives rise to the downshift in the *d*-band center on the PtSn surfaces.

Geometric Effect. Carefully analyzing the adsorption configurations and transition state geometries, we find that the PtSn surfaces are substantially distorted because of their interaction with the C_3 intermediates, especially on the alloys with high Sn contents. For instance, the strong outward relaxations of the bonding metal atom can be observed in the geometries, as shown in Figure 2. In the earlier computational studies, the surface deformation induced by ethylene adsorption was found to dramatically affect the adsorption energy.[64] To analyze the direct interaction strength between the adsorbates and the PtSn alloyed surfaces, the adsorption energies of propane, propyl, and propylene are decomposed according to the scheme suggested by Haubrich et al.:[65]

$$E_{ads} = E_{def,surface} + E_{def,adsorbate} + E_{bin} \quad (6)$$

where $E_{def,surface}$ and $E_{def,\ adsorbate}$ are the deformation energies of the metal surface and adsorbed species, which are defined as the total energy difference of the bare surface and isolated fragment before and after adsorption, respectively; E_{bin} is the direct binding energy between the metal surface and the adsorbate, which reflects the intrinsic affinity of metal for hydrocarbon. The decomposition of the adsorption energies of propane, propyl, and propylene on the Pt and PtSn surfaces are summarized in Figure 10a. Furthermore, to figure out the

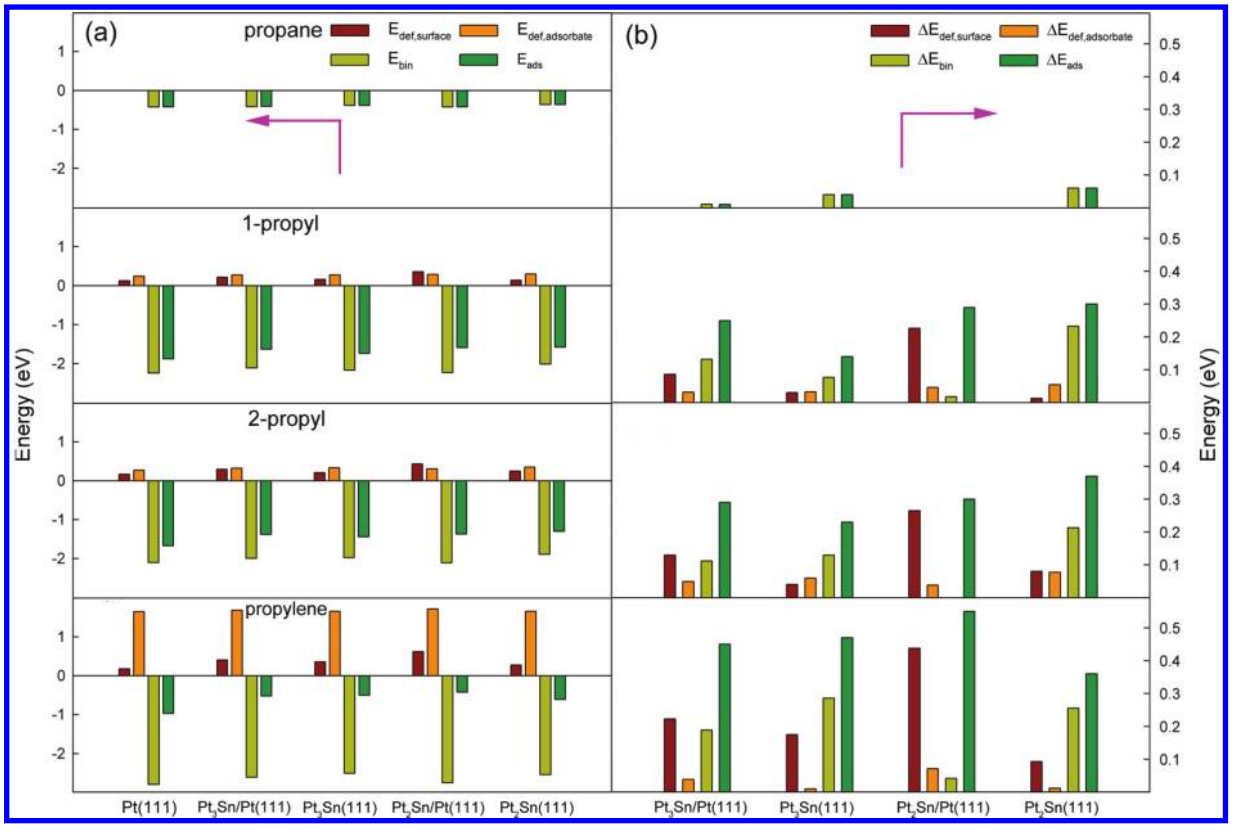

Figure 10. (a) Decomposition of the adsorption energies of propane, propyl, and propylene on the Pt and PtSn surfaces. (b) Changes in E_{ads}, $E_{def,surface}$, $E_{def,adsorbate}$, and E_{bin} with respect to the data on Pt(111).

dx.doi.org/10.1021/cs300031d | *ACS Catal.* 2012, 2, 1247−1258

dominant factor in determining the variation in the adsorption energy, the changes in E_{ads}, $E_{def,surface}$, $E_{def,\ adsorbate}$, and E_{bin} are calculated with respect to the data on Pt(111) and are given in Figure 10b.

From Figure 10a, one can see the deformation energies are positive and have a negative effect on the binding of the C_3 species. As for propane the deformation energies of both the surface and the adsorbate are negligible because the propane molecule is physisorbed and the force between the surface and the adsorbate is rather small. Consequently, the binding energies are very close to the adsorption energies. Unlike the situation in propane, the adsorption of 1-propyl and 2-propyl on all the surfaces gives rise to considerable surface and adsorbate deformation. Nevertheless, the magnitudes of the two comparable deformation energies (the energy difference is within 0.15 eV) remain much lower than those of the binding energies.

The binding energy of propylene ranges from −2.51 eV to −2.79 eV, which is much higher than its adsorption energy. Earlier theoretical studies have reported similar binding energies for ethylene and propylene adsorption on the Pt and PtSn surfaces, and the energy difference is within 0.20 eV on different surfaces.[16,65] The molecular deformation energies are in the region of 1.64−1.71 eV, much higher than those of propyl and consistent with the data reported by Nykänen and Honkala.[16] This is because the distorted propylene molecule loses its "planarity" as the C−H bonds bend away from the surface plane and simultaneously the C═C double bond is stretched by 0.15 Å. The surface deformation energies are below 0.62 eV, which are only 10−30% of the molecule deformation and binding energies.

Comparing the decomposed variations shown in Figure 10b, one can see that the change in the surface deformation energy is the dominant factor that determines the variation in the adsorption energy on the surface alloys, while on the bulk alloys the change in the binding energy make a major contribution.

Surface Coverage Effect. The surface coverage of reactive intermediates is another important factor that has an effect on reaction rates. In experiments, hydrocarbons (C_3H_x) and atomic H were observed to be coadsorbed on the Pt catalyst in propane dehydrogenation.[12,26,27] Since the coadsorption would lower the bonding ability of surface metal atoms by deactivating the metal *d*-states,[66] the increase in surface coverage is expected to promote propylene desorption and to benefit the selectivity toward propylene.

To quantify the surface coverage effect, we performed calculations to obtain the kinetic parameters for the dehydrogenation process from propane to propylene on both the bare and the H-covered Pt_3Sn alloy surfaces at the surface coverage of 1/4 ML. For example, the energy barrier for the activation of propane on $Pt_3Sn(111)$ increases by 0.30 eV. In the presence of H, the dehydrogenation is further inhibited, while the desorption of propylene is promoted by a lower energy barrier, implying that the selectivity toward propylene on the PtSn surfaces would be significantly improved at the expense of a lower catalytic activity for propane dehydrogenation under realistic experimental conditions.

At high surface coverage, the C−C bond cleavage would also be suppressed. On one hand, high surface coverage makes it difficult to achieve a large ensemble which is essential to activate cracking reactions because extra surface vacant sites are required to accommodate detached fragments. On the other hand, the lateral interaction weakens the binding of the final products more greatly than that of the initial state because of the surface-mediated bonding competition effect, and therefore the reaction enthalpy is reduced.[67] According to the BEP relationship,[55] it can be deduced that the activation energy for the cracking of hydrocarbons increases at higher surface coverage, which in turn gives rise to smaller amount of side products.

Catalytic Role of Sn. As aforementioned, the introduction of Sn can weaken the binding strength of hydrocarbons and suppress the bond breaking reactions on the Pt surface, leading to a lower catalytic activity but a higher selectivity toward propylene. The catalytic properties of the PtSn alloyed surfaces are attributed to the modification of the *d*-band of surface Pt atoms by adjacent Sn atoms. Our DFT results are well supported by the experimental observations in the PtSn bimetallic catalytic system. For example, Berndt et al. reported that the catalytic activity for cyclohexane dehydrogenation on the PtSn catalyst is reduced by 44% compared to Pt.[25] Moreover, Yarusov et al. further found that the catalytic activity of the PtSn catalyst is inversely proportional to the content of Sn by comparing the catalytic activities for dehydrogenation on different PtSn alloys.[24] As a result of the promotion of propylene desorption by Sn, the selectivity toward propylene on PtSn alloys was about 10% higher than that on Pt.[1] Simultaneously, as the deep dehydrogenation of the C_3 intermediates is eliminated, coke formation is suppressed and the long-term stability of the PtSn catalyst is achieved.

CONCLUSION

DFT calculations have been performed to investigate the effect of Sn on the catalytic activity and selectivity of Pt catalyst in propane dehydrogenation. Five models with different Sn to Pt surface molar ratios are constructed to represent the PtSn surfaces. Propane is found to be physisorbed on the Pt and PtSn surfaces with similar binding strength, while the adsorption energies of propyl and propylene become less negative with increasing Sn content. Through electronic structure calculations, it is found that the alloying of Pt with less reactive Sn leads to the increase in the *d*-bandwidth, which gives rise to the downshift in the *d*-band center on the PtSn surfaces. With the decomposition of the adsorption energy, the change in the surface deformation energy is predicted to be the dominant factor that determines the variation in the adsorption energy on the surface alloys, while on the bulk alloys the change in the binding energy makes a major contribution.

On all the alloyed surfaces the introduction of Sn has a minor effect on the geometries of transition states for the dehydrogenation reactions. Alloying Pt with Sn will significantly lower the reaction rate of propane dehydrogenation, and the variation in the energy barriers depends strongly on the change in the binding strength of H in the geometry of the transition state.

Analyzing the competition between the activation of the C−H bond and the C−C bond for each intermediate, we find that the cracking of these four species is kinetically hindered because of the much higher energy barriers. The deposition of Sn makes it difficult to achieve a large ensemble which is essential to activate cracking reactions because extra surface vacant sites are required to accommodate detached fragments.

The introduction of Sn lowers the desorption barrier for propylene to the gas phase and simultaneously increases the energy barrier for propylene dehydrogenation. As the Sn content increases, the selectivity toward propylene desorption

is significantly improved. Considering the compromise between the catalytic activity and the selectivity, the Pt_3Sn bulk alloy is the best candidate for propane dehydrogenation.

■ ASSOCIATED CONTENT

Supporting Information

Segregation energy of the PtSn alloys with different Sn contents; Activation barriers and adsorption energies for propane dehydrogenation on Pt_3Sn surfaces at high coverages; Computational details of the equilibrium constants for propylene adsorption. This material is available free of charge via the Internet at http://pubs.acs.org.

■ AUTHOR INFORMATION

Corresponding Author

*E-mail: yanzhu@ecust.edu.cn (Y.-A.Z.), chen@nt.ntnu.no (D.C.). Phone: +86 21 6425 3072 (Y.-A.Z.), +47 73593149 (D.C.). Fax: +86 21 6425 3528 (Y.-A.Z.), +47 48222428 (D.C.).

Funding

This research is supported by Natural Science Foundation of China (No. 21003046) and 973 Project of Ministry of Science and Technology of China (No. 2012CB720500).

Notes

The authors declare no competing financial interest.

■ ACKNOWLEDGMENTS

Ming-Lei Yang would like to thank Prof. Graeme Henkelman for discussion and the use of computational resources at UT-Austin.

■ REFERENCES

(1) Bariås, O. A.; Holmen, A.; Blekkan, E. A. *J. Catal.* **1996**, *158*, 1–12.
(2) Delbecq, F.; Sautet, P. *J. Catal.* **2003**, *220*, 115–126.
(3) Kumar, M. S.; Chen, D.; Holmen, A.; Walmsley, J. C. *Catal. Today* **2009**, *142*, 17–23.
(4) Laref, S.; Delbecq, F.; Loffreda, D. *J. Catal.* **2009**, *265*, 35–42.
(5) Vigné, F.; Haubrich, J.; Loffreda, D.; Sautet, P.; Delbecq, F. *J. Catal.* **2010**, *275*, 129–139.
(6) Nawaz, Z.; Tang, X.; Zhang, Q.; Wang, D.; Fei, W. *Catal. Commun.* **2009**, *10*, 1925–1930.
(7) Pisduangdaw, S.; Panpranot, J.; Methastidsook, C.; Chaisuk, C.; Faungnawakij, K.; Praserthdam, P.; Mekasuwandumrong, O. *Appl. Catal., A* **2009**, *370*, 1–6.
(8) Lobera, M. P.; Téllez, C.; Herguido, J.; Menéndez, M. *Appl. Catal., A* **2008**, *349*, 156–164.
(9) Biloen, P.; Helle, J. N.; Sachtler, W. M. H. *J. Catal.* **1979**, *58*, 95–107.
(10) Ribeiro, F. H.; Bonivardi, A. L.; Kim, C.; Somorjai, G. A. *J. Catal.* **1994**, *150*, 186–198.
(11) Cortright, R. D.; Dumesic, J. A. *J. Catal.* **1994**, *148*, 771–778.
(12) Kumar, M. S.; Chen, D.; Walmsley, J. C.; Holmen, A. *Catal. Commun.* **2008**, *9*, 747–750.
(13) Larsson, M.; Hultén, M.; Blekkan, E. A.; Andersson, B. *J. Catal.* **1996**, *164*, 44–53.
(14) Völter, J.; Lietz, G.; Uhlemann, M.; Hermann, M. *J. Catal.* **1981**, *68*, 42–50.
(15) Valcárcel, A.; Ricart, J. M.; Clotet, A.; Ilas, F.; Markovits, A.; Minot, C. *J. Catal.* **2006**, *241*, 115–122.
(16) Nykänen, L.; Honkala, K. *J. Phys. Chem. C* **2011**, *115*, 9578–9586.
(17) Tsai, Y. L.; Xu, C.; Koel, B. E. *Surf. Sci.* **1997**, *385*, 37–59.
(18) Zaera, F.; Chrysostomou, D. *Surf. Sci.* **2000**, *457*, 71–88.
(19) Yang, M. L.; Zhu, Y. A.; Fan, C.; Sui, Z. J.; Chen, D.; Zhou, X. G. *J. Mol. Catal. A: Chem.* **2010**, *321*, 42–49.
(20) Yang, M. L.; Zhu, Y. A.; Fan, C.; Sui, Z. J.; Chen, D.; Zhou, X. G. *Phys. Chem. Chem. Phys.* **2011**, *13*, 3257–3267.
(21) Vajda, S.; Pellin, M. J.; Greeley, J. P.; Marshall, C. L.; Curtiss, L. A.; Ballentine, G. A.; Elam, J. W.; Catillon-Mucherie, S.; Redfern, P. C.; Mehmood, F.; Zapol, P. *Nat. Mater.* **2009**, *8*, 213–216.
(22) Biloen, P.; Dautzenberg, F. M.; Sachtler, W. M. H. *J. Catal.* **1977**, *50*, 77–86.
(23) Suzuki, I.; Kaneko, Y. *J. Catal.* **1977**, *47*, 239–248.
(24) Yarusov, I. B.; Zatolokina, E. V.; Shitova, N. V.; Belyi, A. S.; Ostrovskii, N. M. *Catal. Today* **1992**, *13*, 655–658.
(25) Berndt, H.; Mehner, H.; Völter, J.; Meisel, W. *Z. Anorg. Allg. Chem.* **1977**, *429*, 47–58.
(26) Anson, C. E.; Sheppard, N.; Bender, B. R.; Norton, J. R. *J. Am. Chem. Soc.* **1999**, *121*, 529–534.
(27) Burnett, D. J.; Gabelnick, A. M.; Marsh, A. L.; Fischer, D. A.; Gland, J. L. *Surf. Sci.* **2004**, *553*, 1–12.
(28) Kresse, G.; Furthmüller, J. *Comput. Mater. Sci.* **1996**, *6*, 15–50.
(29) Kresse, G.; Furthmüller, J. *Phys. Rev. B* **1996**, *54*, 11169–11186.
(30) Kresse, G.; Hafner, J. *Phys. Rev. B* **1993**, *48*, 13115–13118.
(31) Perdew, J. P.; Burke, K.; Ernzerhof, M. *Phys. Rev. Lett.* **1996**, *77*, 3865–3868.
(32) Blöchl, P. E. *Phys. Rev. B* **1994**, *50*, 17953–17979.
(33) Methfessel, M.; Paxton, A. T. *Phys. Rev. B* **1989**, *40*, 3616–3621.
(34) Atrei, A.; Bardi, U.; Wu, J. X.; Zanazzi, E.; Rovida, G. *Surf. Sci.* **1993**, *290*, 286–294.
(35) Paffett, M. T.; Windham, R. G. *Surf. Sci.* **1989**, *208*, 34–54.
(36) Hoheisel, M.; Speller, S.; Kuntze, J.; Atrei, A.; Bardi, U.; Heiland, W. *Phys. Rev. B* **2001**, *63*, 245403.
(37) Kuntze, J.; Speller, S.; Heiland, W.; Atrei, A.; Spolveri, I.; Bardi, U. *Phys. Rev. B* **1998**, *58*, R16005.
(38) Galeotti, M.; Atrei, A.; Bardi, U.; Rovida, G.; Torrini, M. *Surf. Sci.* **1994**, *313*, 349–354.
(39) Pick, S. *Surf. Sci.* **1999**, *436*, 220–226.
(40) Llorca, J.; Homs, N.; Fierro, J.-L. G.; Sales, J.; Piscina, P. R. d. l. *J. Catal.* **1997**, *166*, 44–52.
(41) Ohnishi, N.; Yoshida, S.; Namba, Y. *Mater. Trans.* **2006**, *47*, 267–270.
(42) Henkelman, G.; Jonsson, H. *J. Chem. Phys.* **1999**, *111*, 7010–7022.
(43) Henkelman, G.; Jonsson, H. *J. Chem. Phys.* **2001**, *115*, 9657–9666.
(44) Olsen, R. A.; Kroes, G. J.; Henkelman, G.; Arnaldsson, A.; Jonsson, H. *J. Chem. Phys.* **2004**, *121*, 9776–9792.
(45) McMaster, M. C.; Arumainayagam, C. R.; Madix, R. J. *Chem. Phys.* **1993**, *177*, 461–472.
(46) Cushing, G. W.; Navin, J. K.; Donald, S. B.; Valadez, L.; Johanek, V.; Harrison, I. *J. Phys. Chem. C* **2010**, *114*, 17222–17232.
(47) Kao, C. L.; Madix, R. J. *Surf. Sci.* **2004**, *557*, 215–230.
(48) Lee, K.; Murray, a. D.; Kong, L.; Lundqvist, B. I.; Langreth, D. C. *Phys. Rev. B* **2010**, *82*, 081101.
(49) Dion, M.; Rydberg, H.; Schröder, E.; Langreth, D. C.; Lundqvist, B. I. *Phys. Rev. Lett.* **2004**, *92*, 246401.
(50) Chesters, M. A.; Gardner, P.; McCash, E. M. *Surf. Sci.* **1989**, *209*, 89–99.
(51) Fosser, K. A.; Kang, J. H.; Nuzzo, R. G.; Wöll, C. *J. Chem. Phys.* **2007**, *126*, 194707.
(52) Fosser, K. A.; Nuzzo, R. G.; Bagus, P. S.; Wöll, C. *Angew. Chem., Int. Ed.* **2002**, *41*, 1735–1737.
(53) Brönsted, J. N. *Chem. Rev.* **1928**, *5*, 231–338.
(54) Evans, M. G.; Polanyi, M. *Trans. Faraday Soc.* **1938**, *34*, 11–24.
(55) Bligaard, T.; Nørskov, J. K.; Dahl, S.; Matthiesen, J.; Christensen, C. H.; Sehested, J. *J. Catal.* **2004**, *224*, 206–217.
(56) Koestner, R.; Frost, J.; Stair, P.; Hove, M. V.; Somorjai, G. *Surf. Sci.* **1982**, *116*, 85–103.
(57) Michaelides, A.; Hu, P. *J. Am. Chem. Soc.* **2000**, *122*, 9866–9867.
(58) Michaelides, A.; Hu, P. *J. Chem. Phys.* **2001**, *114*, 5792–5795.
(59) Michaelides, A.; Hu, P. *J. Chem. Phys.* **2001**, *114*, 2523–2526.

(60) Hammer, B. *Surf. Sci.* **2000**, *459*, 323−348.
(61) Goda, A. M.; Barteau, M. A.; Chen, J. G. *J. Phys. Chem. B* **2006**, *110*, 11823−11831.
(62) Ruban, A.; Hammer, B.; Stoltze, P.; Skriver, H. L.; Nørskov, J. K. *J. Mol. Catal. A: Chem.* **1997**, *115*, 421−429.
(63) Kitchin, J. R.; Nørskov, J. K.; Barteau, M. A.; Chen, J. G. *J. Chem. Phys.* **2004**, *120*, 10240−10246.
(64) Watson, G. W.; Wells, R. P. K.; Willock, D. J.; Hutchings, G. J. *Surf. Sci.* **2000**, *459*, 93−103.
(65) Haubrich, J.; Becker, C.; Wandelt, K. *Surf. Sci.* **2009**, *603*, 1476−1485.
(66) Hammer, B.; Nørskov, J. K. *Adv. Catal.* **2000**, *45*, 71−129.
(67) Liu, Z. P.; Hu, P.; Lee, M. H. *J. Chem. Phys.* **2003**, *119*, 6282−6289.